# Supplementary Material: "Time-Discrete Parameter Identification Algorithms for Two Deterministic Epidemiological Models applied to the Spread of COVID-19"

**Benjamin Wacker**[1,*]**, Marc Timme**[2,3]**, and Jan Schlüter**[1,3]

[1]Next Generation Mobility Group, Max-Planck-Institut for Dynamics and Self-Organization, Department of Dynamics of Complex Fluids, Am Fassberg 17, D-37077 Göttingen, Germany
[2]Chair for Network Dynamics, Cluster of Excellence Physics of Life, Institute for Theoretical Physics and Center for Advancing Electronics Dresden (cfaed), Technical University of Dresden, Helmholtzstr. 18, D-01069 Dresden, Germany
[3]Institute for Dynamics of Complex Systems, Faculty of Physics, Georg-August-University of Göttingen, Friedrich-Hund-Platz 1, D-37077 Göttingen, Germany
[*]Corresponding author: Benjamin Wacker

## ABSTRACT

We portray further results on our parameter identification algorithms for SIR and SIRD models in this supplementary material. Our investigations include France, Germany, Italy, Spain, Sweden and the United States. We consider a time period ranging from 22 January, 2020 to 30 April, 2020. That corresponds exactly to one hundred days. For calculation of arithmetic means and medians, we delete some outliers and set different ranges for the time periods depending on the considered country. We refer interested readers to our main document and our statement on code availability for further details.
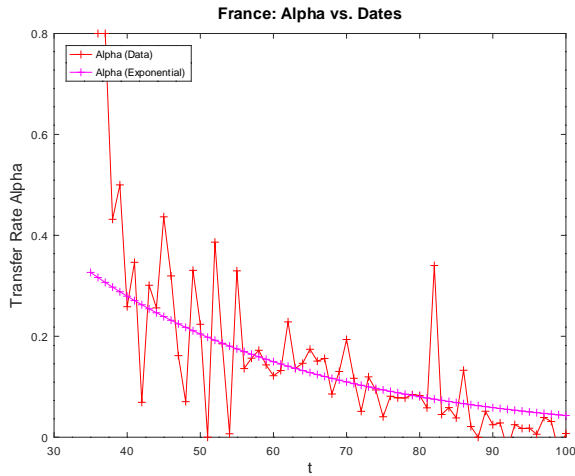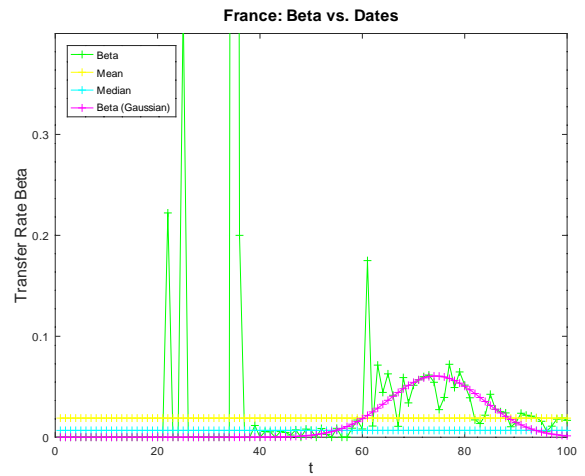
# Results for France
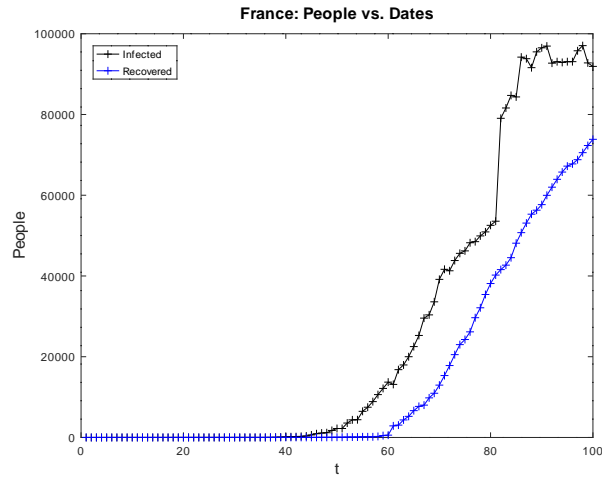


(a) Grouped Plots
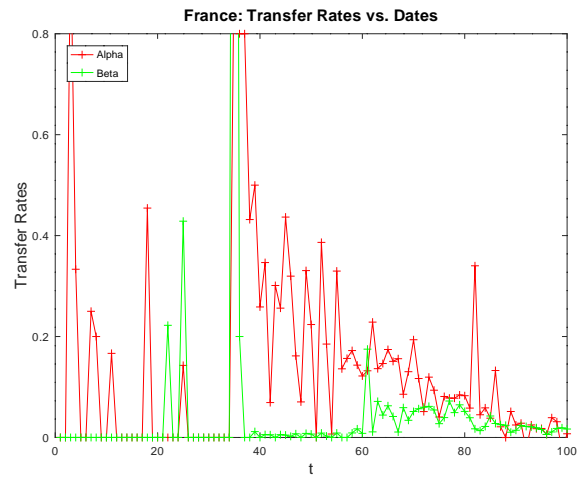


(b) Transfer Rates



(c) Contact Rate



(d) Recovery Rate

**Figure 1.** Results for our time-discrete parameter identification SIR model. (a) Plots of processed data for infected people and (cumulative) recovered people at time $t$. (b) Plots of both time-varying transfer rates $\alpha(t)$ and $\beta(t)$ from our identification algorithm. (c) Plots of time-varying contact rate $\alpha(t)$ and a parametric approximation with a decaying exponential function as a model. (d) Plots of time-varying recovery rate $\beta(t)$, its mean and median and a parametric approximation with a Gaussian function.
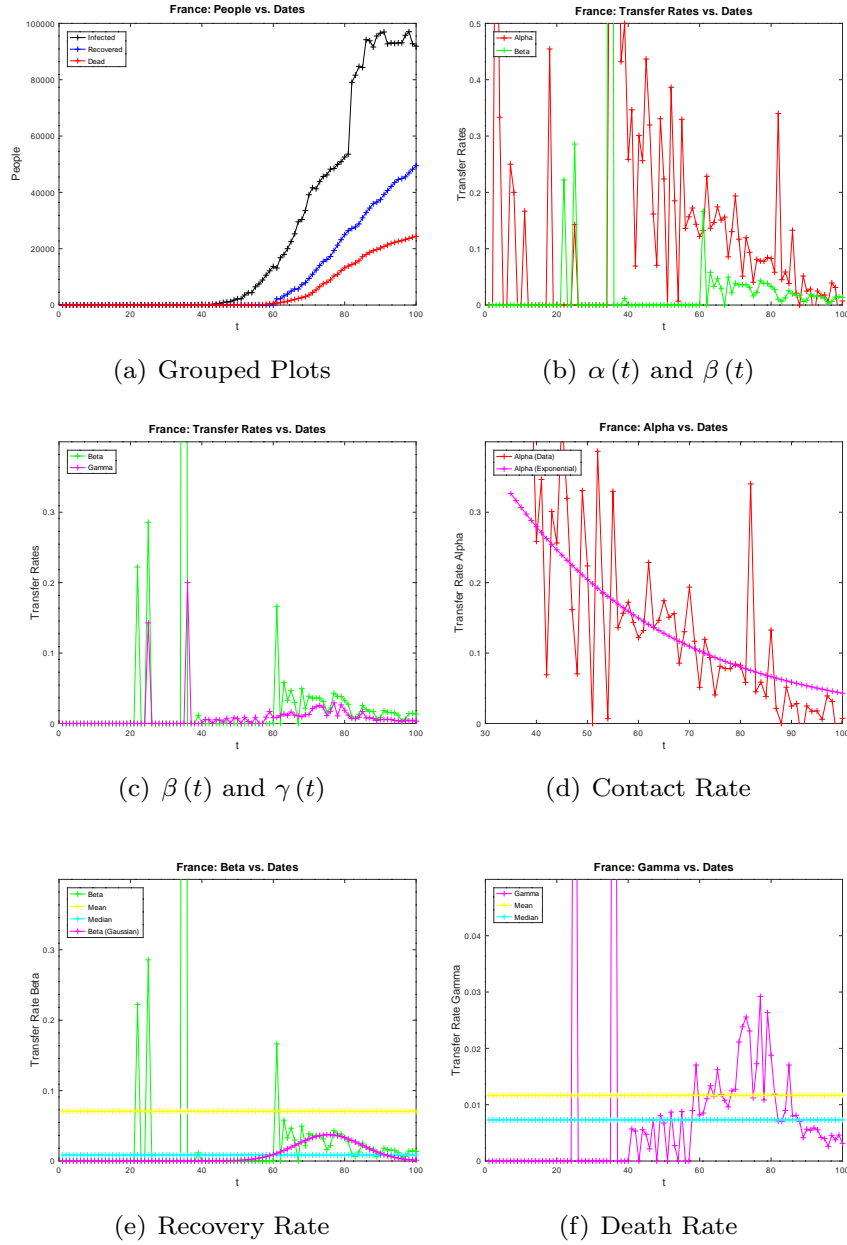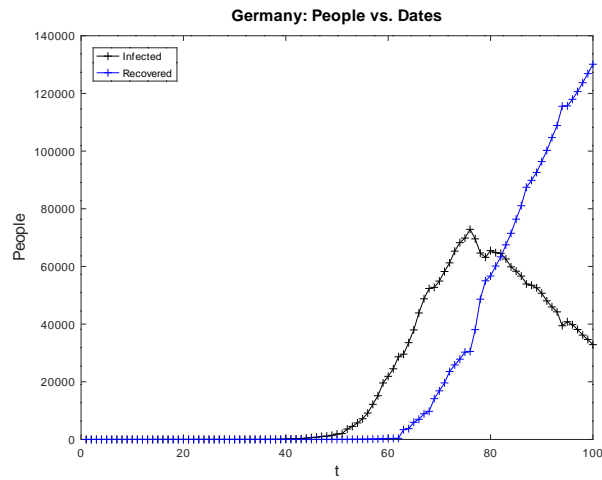
(a) Grouped Plots

(b) $\alpha(t)$ and $\beta(t)$

(c) $\beta(t)$ and $\gamma(t)$

(d) Contact Rate

(e) Recovery Rate

(f) Death Rate

**Figure 2.** Results for our time-discrete parameter identification SIRD model. (a) Plots of processed data for infected people, (cumulative) recovered people and (cumulative) dead people at time $t$. (b) Plots of the time-varying transfer rates $\alpha(t)$ and $\beta(t)$ from our identification algorithm. (c) Plots of the time-varying transfer rates $\beta(t)$ and $\gamma(t)$ from our identification algorithm. (d) Plots of time-varying contact rate $\alpha(t)$ and a parametric approximation with a decaying exponential function. (e) Plots of time-varying recovery rate $\beta(t)$, its mean and median and a parametric approximation with a Gaussian function. (f) Plots of time-varying death rate $\gamma(t)$, its mean and its median.
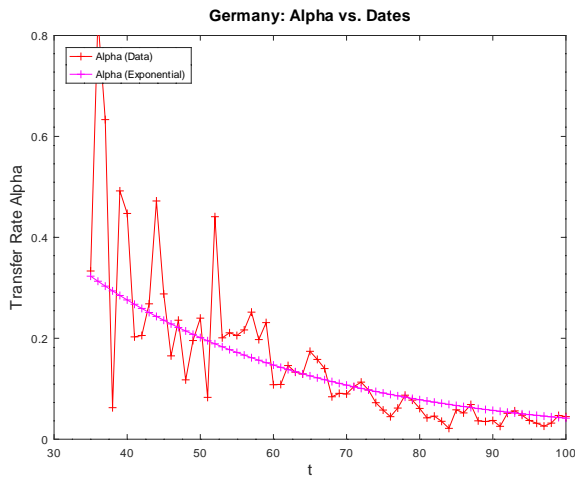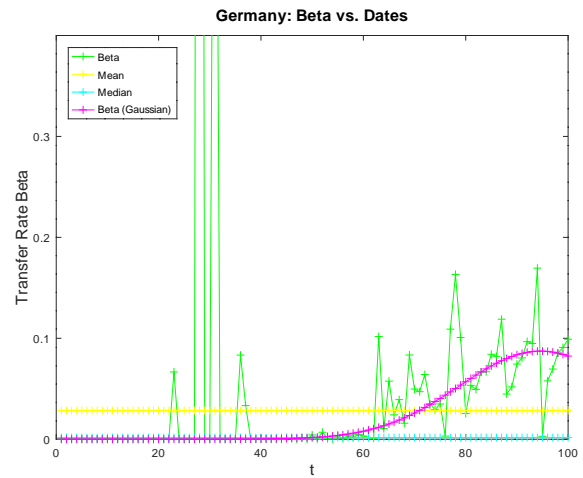
**Results for Germany**



(a) Grouped Plots
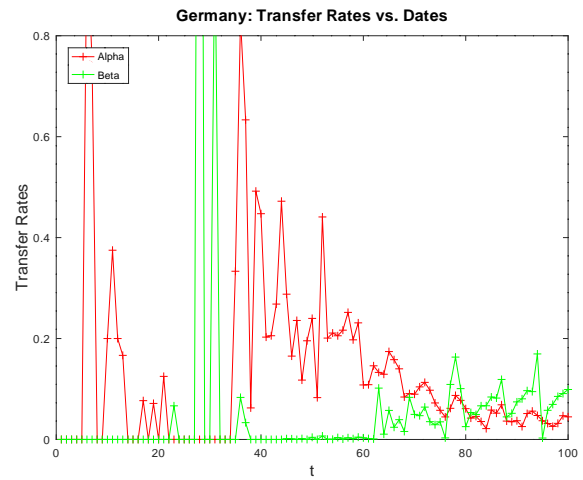


(b) Transfer Rates



(c) Contact Rate



(d) Recovery Rate

**Figure 3.** Results for our time-discrete parameter identification SIR model. (a) Plots of processed data for infected people and (cumulative) recovered people at time $t$. (b) Plots of both time-varying transfer rates $\alpha(t)$ and $\beta(t)$ from our identification algorithm. (c) Plots of time-varying contact rate $\alpha(t)$ and a parametric approximation with a decaying exponential function as a model. (d) Plots of time-varying recovery rate $\beta(t)$, its mean and median and a parametric approximation with a Gaussian function.
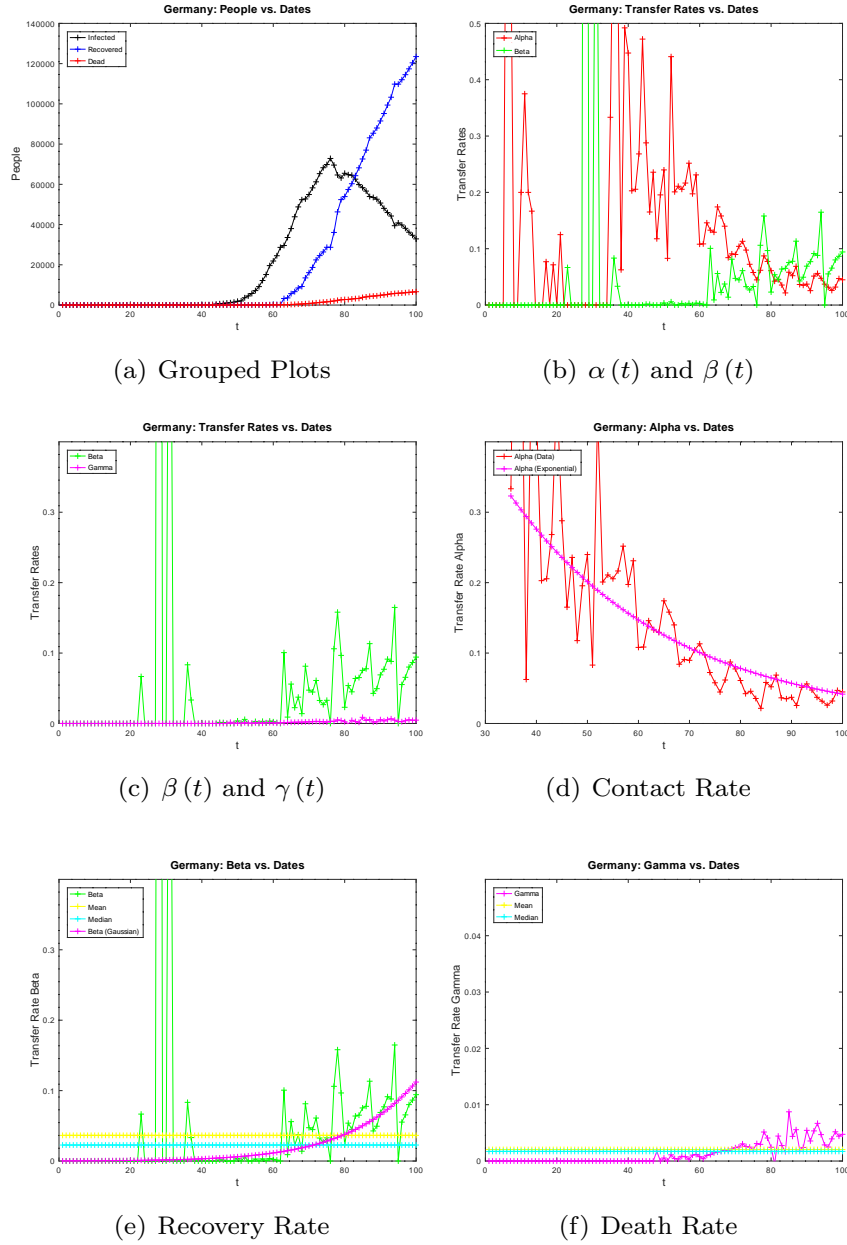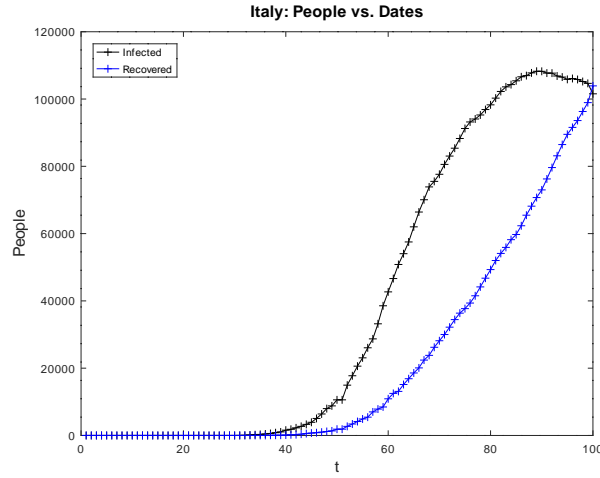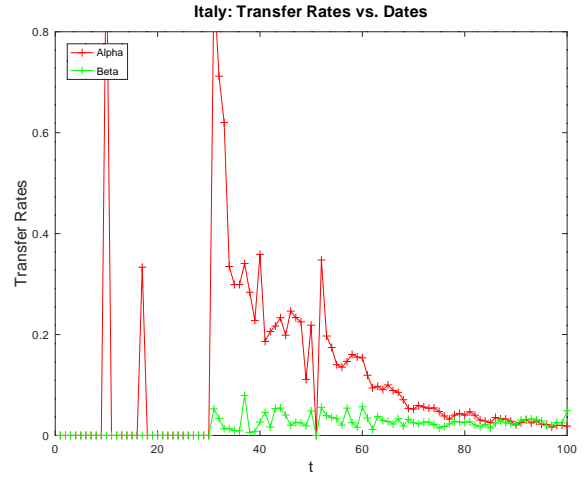
**Figure 4.** Results for our time-discrete parameter identification SIRD model. (a) Plots of processed data for infected people, (cumulative) recovered people and (cumulative) dead people at time $t$. (b) Plots of the time-varying transfer rates $\alpha(t)$ and $\beta(t)$ from our identification algorithm. (c) Plots of the time-varying transfer rates $\beta(t)$ and $\gamma(t)$ from our identification algorithm. (d) Plots of time-varying contact rate $\alpha(t)$ and a parametric approximation with a decaying exponential function. (e) Plots of time-varying recovery rate $\beta(t)$, its mean and median and a parametric approximation with a Gaussian function. (f) Plots of time-varying death rate $\gamma(t)$, its mean and its median.
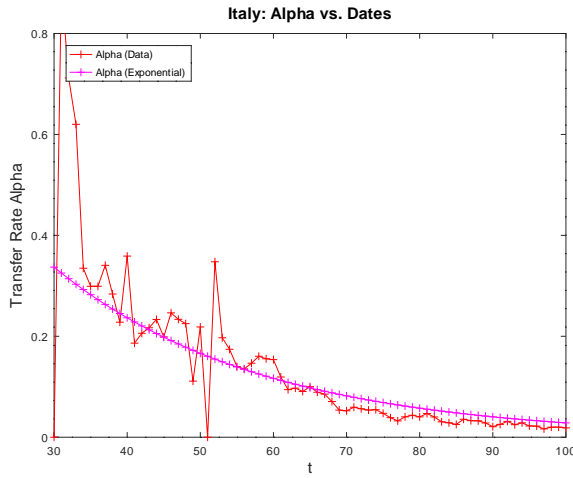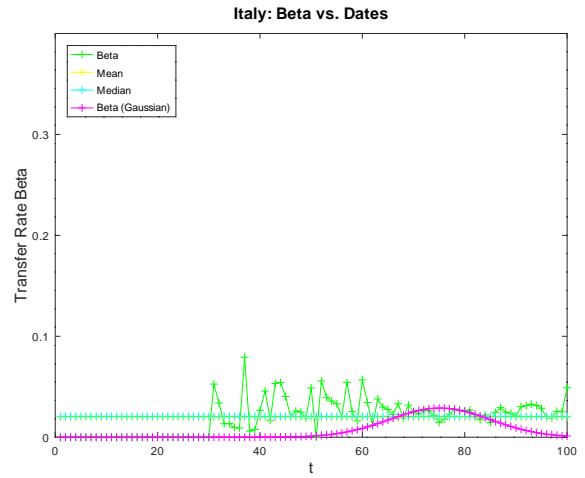
## Results for Italy



(a) Grouped Plots

(b) Transfer Rates

(c) Contact Rate

(d) Recovery Rate

**Figure 5.** Results for our time-discrete parameter identification SIR model. (a) Plots of processed data for infected people and (cumulative) recovered people at time $t$. (b) Plots of both time-varying transfer rates $\alpha(t)$ and $\beta(t)$ from our identification algorithm. (c) Plots of time-varying contact rate $\alpha(t)$ and a parametric approximation with a decaying exponential function as a model. (d) Plots of time-varying recovery rate $\beta(t)$, its mean and median and a parametric approximation with a Gaussian function.
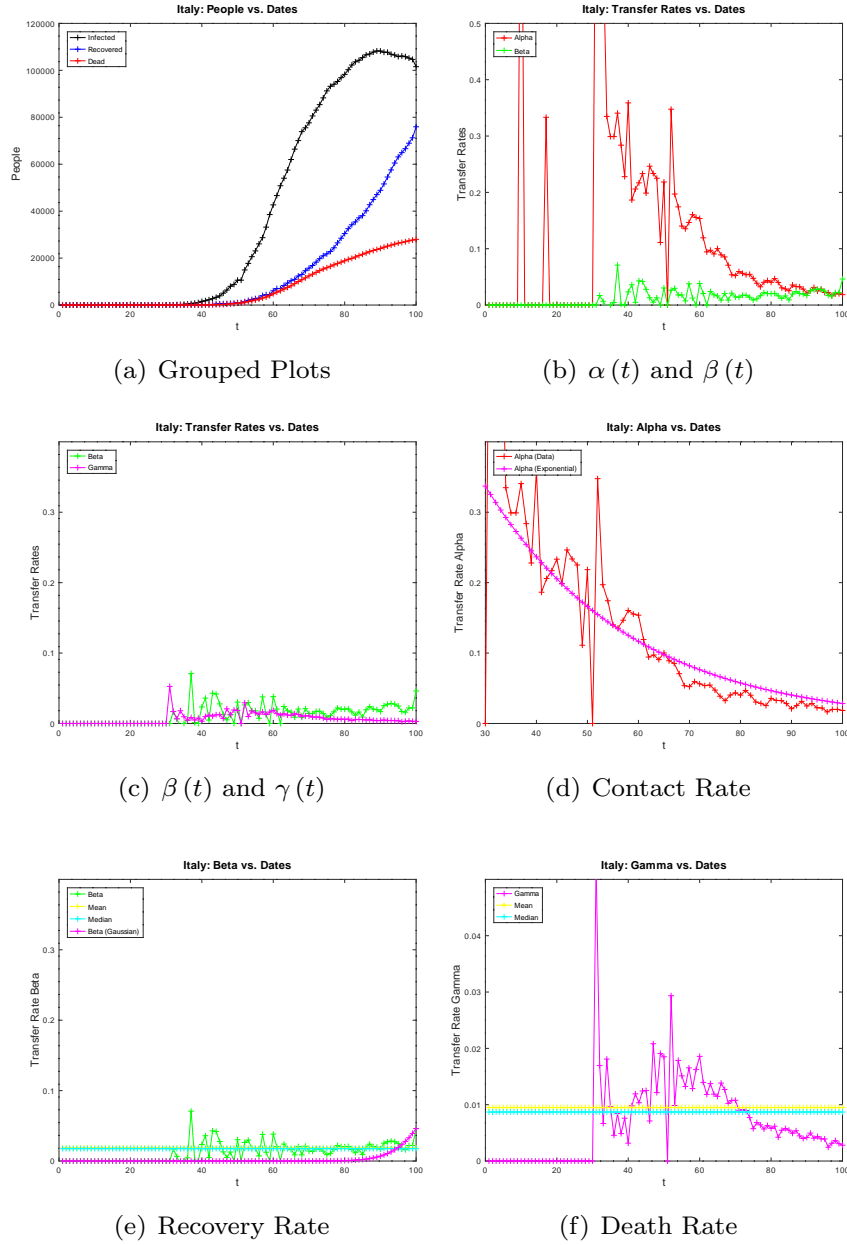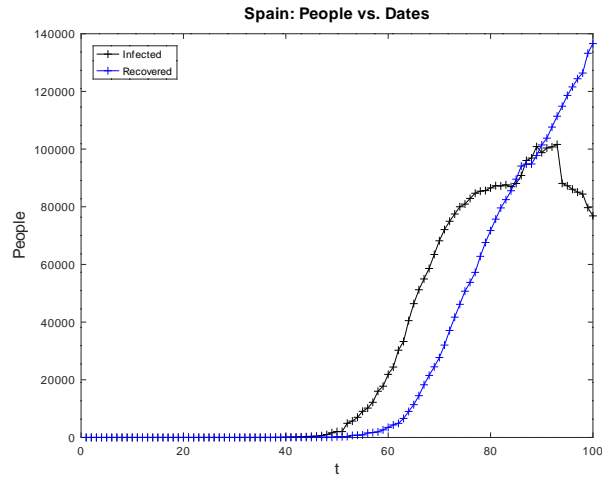
(a) Grouped Plots

(b) $\alpha(t)$ and $\beta(t)$

(c) $\beta(t)$ and $\gamma(t)$

(d) Contact Rate

(e) Recovery Rate

(f) Death Rate

**Figure 6.** Results for our time-discrete parameter identification SIRD model. (a) Plots of processed data for infected people, (cumulative) recovered people and (cumulative) dead people at time $t$. (b) Plots of the time-varying transfer rates $\alpha(t)$ and $\beta(t)$ from our identification algorithm. (c) Plots of the time-varying transfer rates $\beta(t)$ and $\gamma(t)$ from our identification algorithm. (d) Plots of time-varying contact rate $\alpha(t)$ and a parametric approximation with a decaying exponential function. (e) Plots of time-varying recovery rate $\beta(t)$, its mean and median and a parametric approximation with a Gaussian function. (f) Plots of time-varying death rate $\gamma(t)$, its mean and its median.
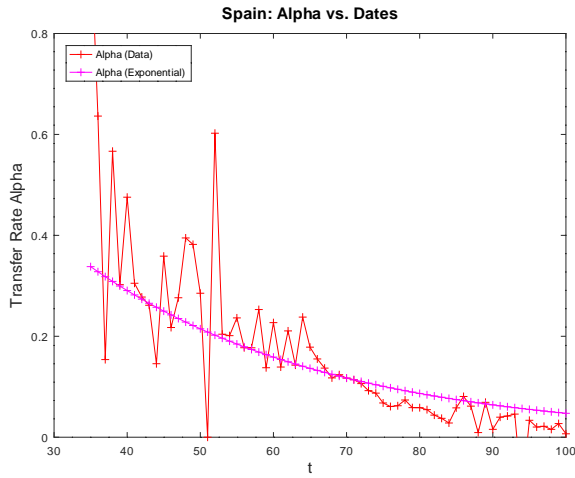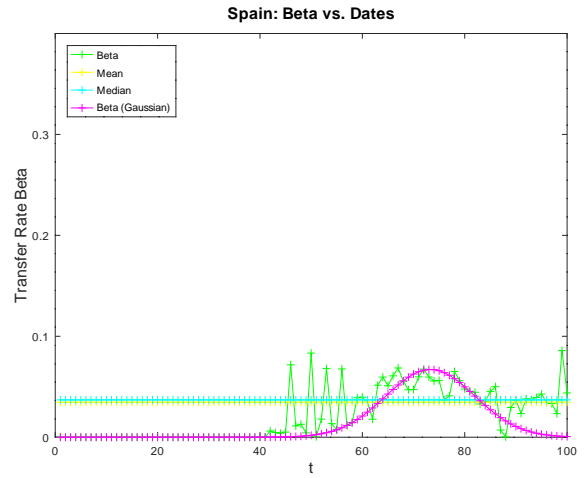
## Results for Spain



(a) Grouped Plots
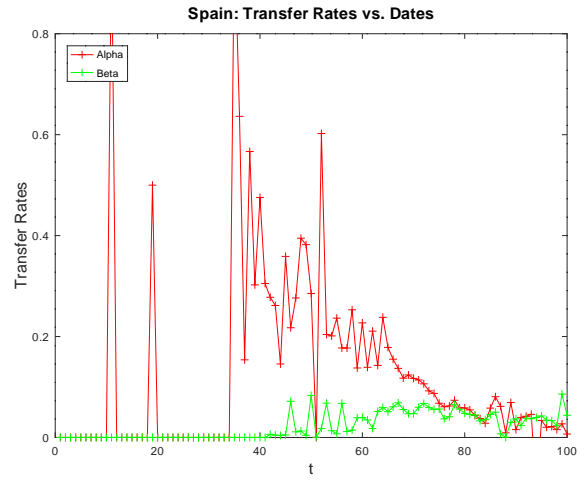
(b) Transfer Rates

(c) Contact Rate

(d) Recovery Rate

**Figure 7.** Results for our time-discrete parameter identification SIR model. (a) Plots of processed data for infected people and (cumulative) recovered people at time $t$. (b) Plots of both time-varying transfer rates $\alpha(t)$ and $\beta(t)$ from our identification algorithm. (c) Plots of time-varying contact rate $\alpha(t)$ and a parametric approximation with a decaying exponential function as a model. (d) Plots of time-varying recovery rate $\beta(t)$, its mean and median and a parametric approximation with a Gaussian function.
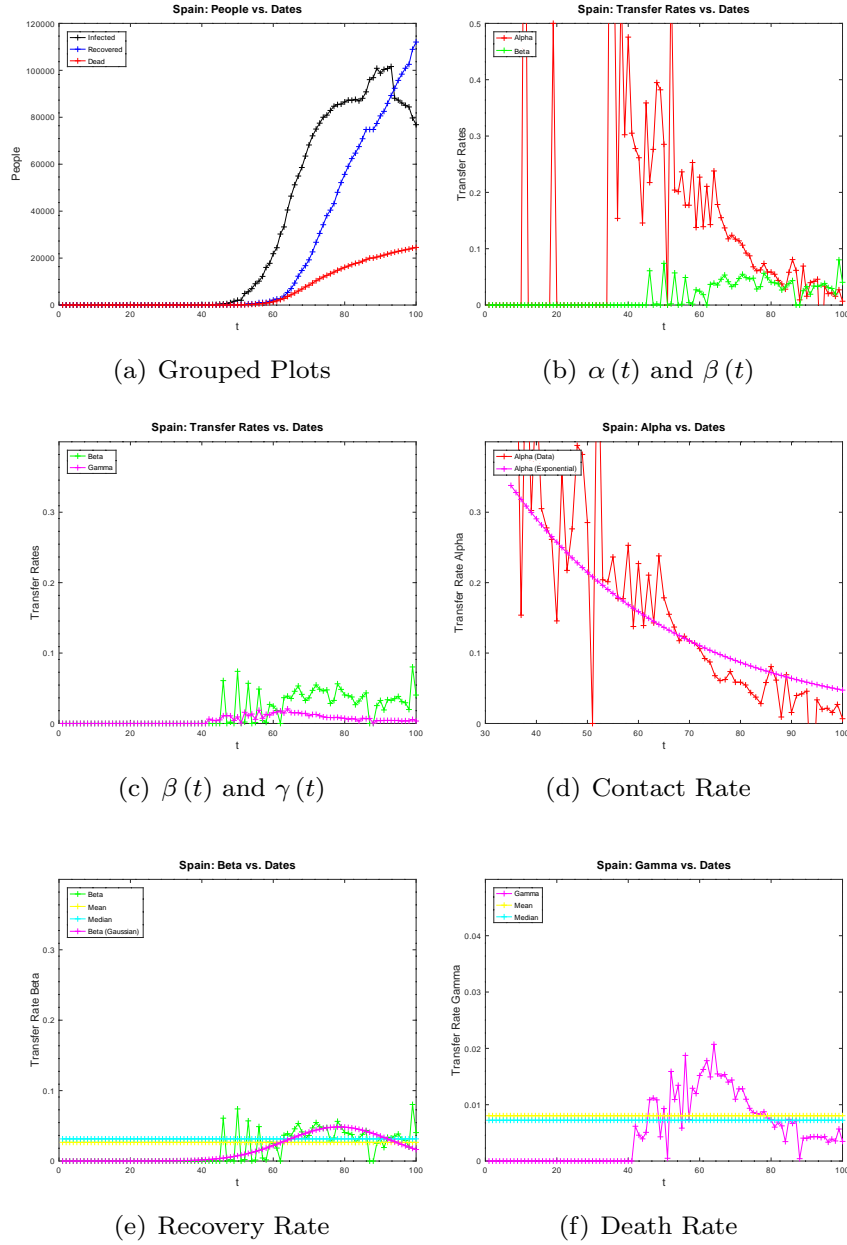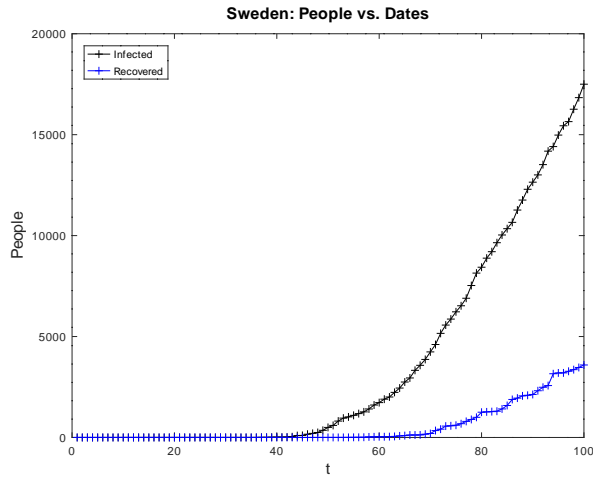
(a) Grouped Plots

(b) $\alpha(t)$ and $\beta(t)$

(c) $\beta(t)$ and $\gamma(t)$

(d) Contact Rate

(e) Recovery Rate

(f) Death Rate

**Figure 8.** Results for our time-discrete parameter identification SIRD model. (a) Plots of processed data for infected people, (cumulative) recovered people and (cumulative) dead people at time $t$. (b) Plots of the time-varying transfer rates $\alpha(t)$ and $\beta(t)$ from our identification algorithm. (c) Plots of the time-varying transfer rates $\beta(t)$ and $\gamma(t)$ from our identification algorithm. (d) Plots of time-varying contact rate $\alpha(t)$ and a parametric approximation with a decaying exponential function. (e) Plots of time-varying recovery rate $\beta(t)$, its mean and median and a parametric approximation with a Gaussian function. (f) Plots of time-varying death rate $\gamma(t)$, its mean and its median.
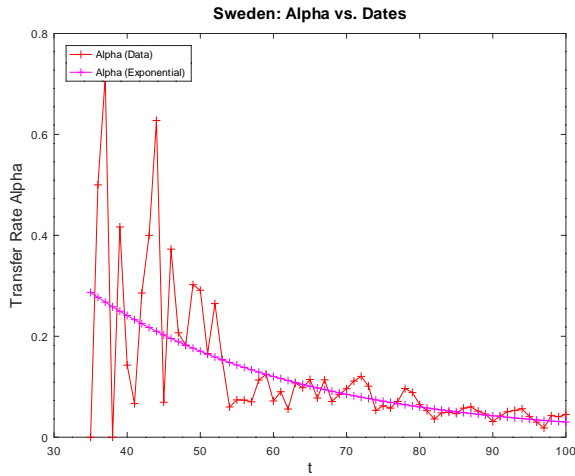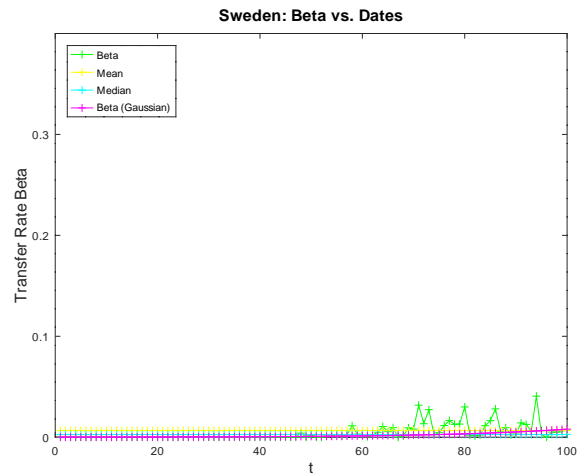
# Results for Sweden



(a) Grouped Plots
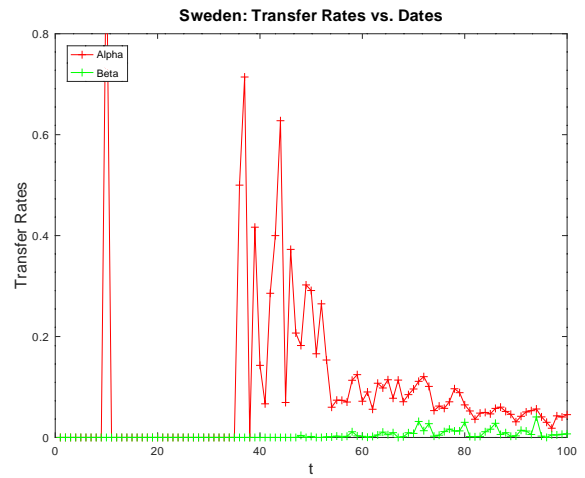


(b) Transfer Rates



(c) Contact Rate



(d) Recovery Rate

**Figure 9.** Results for our time-discrete parameter identification SIR model. (a) Plots of processed data for infected people and (cumulative) recovered people at time $t$. (b) Plots of both time-varying transfer rates $\alpha(t)$ and $\beta(t)$ from our identification algorithm. (c) Plots of time-varying contact rate $\alpha(t)$ and a parametric approximation with a decaying exponential function as a model. (d) Plots of time-varying recovery rate $\beta(t)$, its mean and median and a parametric approximation with a Gaussian function.
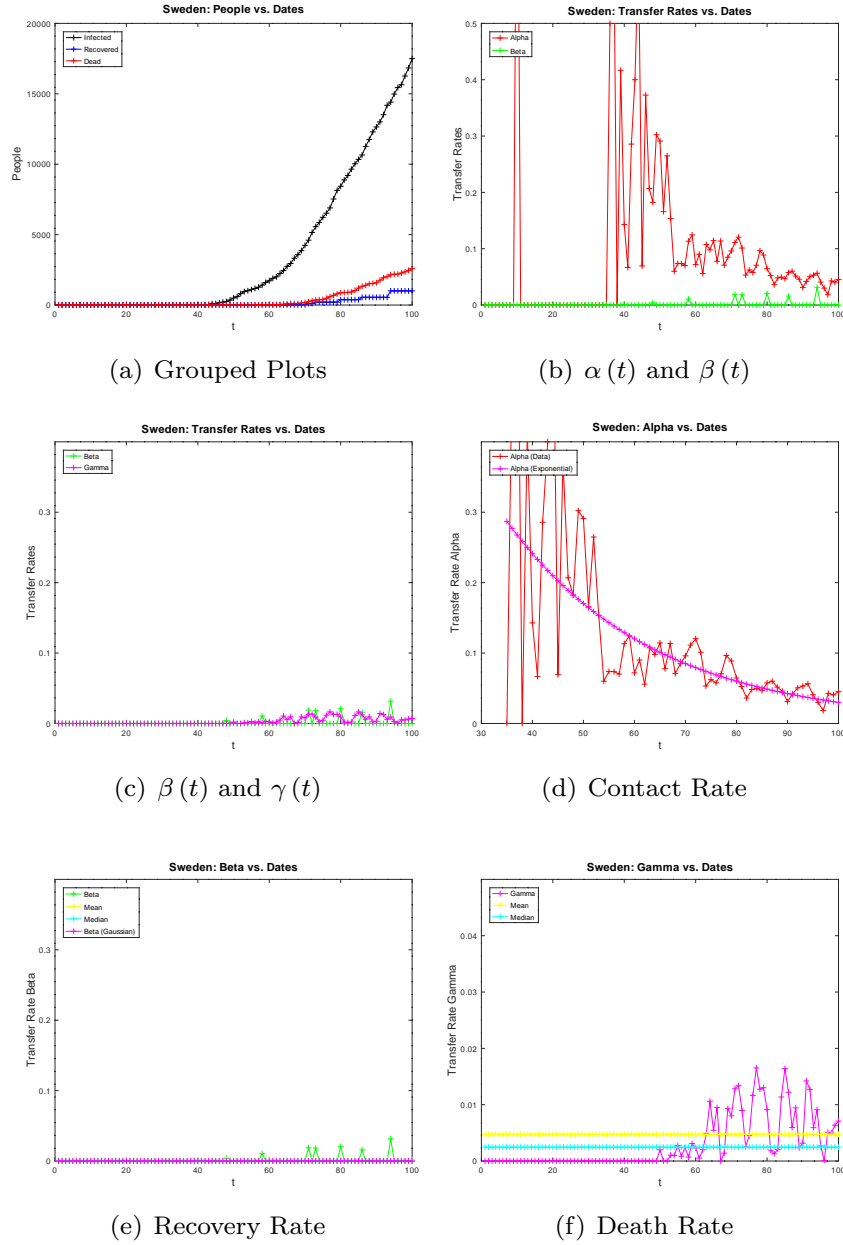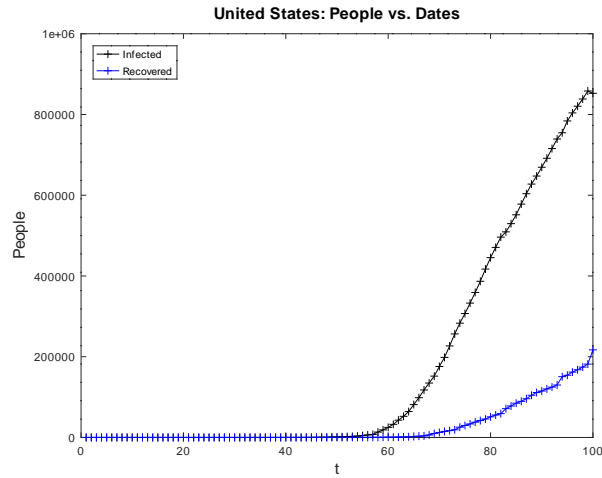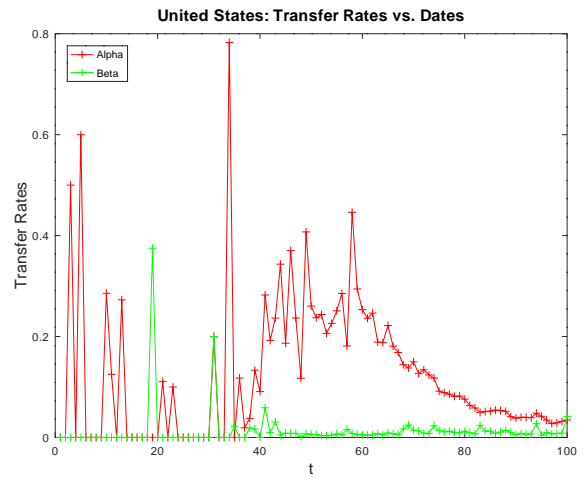
**Figure 10.** Results for our time-discrete parameter identification SIRD model. (a) Plots of processed data for infected people, (cumulative) recovered people and (cumulative) dead people at time $t$. (b) Plots of the time-varying transfer rates $\alpha(t)$ and $\beta(t)$ from our identification algorithm. (c) Plots of the time-varying transfer rates $\beta(t)$ and $\gamma(t)$ from our identification algorithm. (d) Plots of time-varying contact rate $\alpha(t)$ and a parametric approximation with a decaying exponential function. (e) Plots of time-varying recovery rate $\beta(t)$, its mean and median and a parametric approximation with a Gaussian function. (f) Plots of time-varying death rate $\gamma(t)$, its mean and its median.
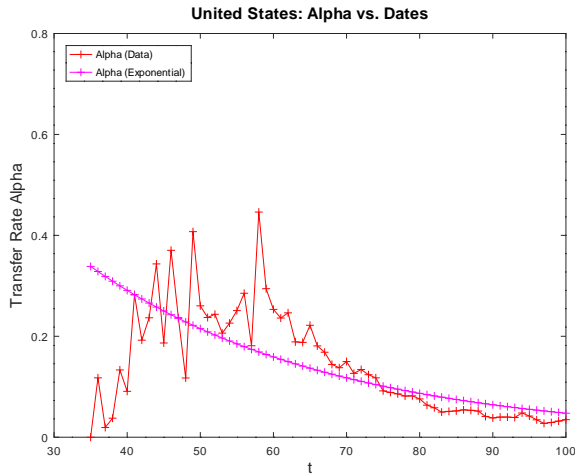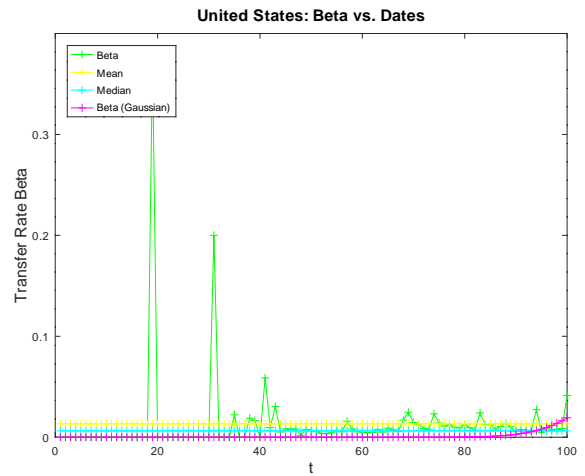
**Results for the United States**



(a) Grouped Plots

(b) Transfer Rates

(c) Contact Rate

(d) Recovery Rate

**Figure 11.** Results for our time-discrete parameter identification SIR model. (a) Plots of processed data for infected people and (cumulative) recovered people at time $t$. (b) Plots of both time-varying transfer rates $\alpha(t)$ and $\beta(t)$ from our identification algorithm. (c) Plots of time-varying contact rate $\alpha(t)$ and a parametric approximation with a decaying exponential function as a model. (d) Plots of time-varying recovery rate $\beta(t)$, its mean and median and a parametric approximation with a Gaussian function.
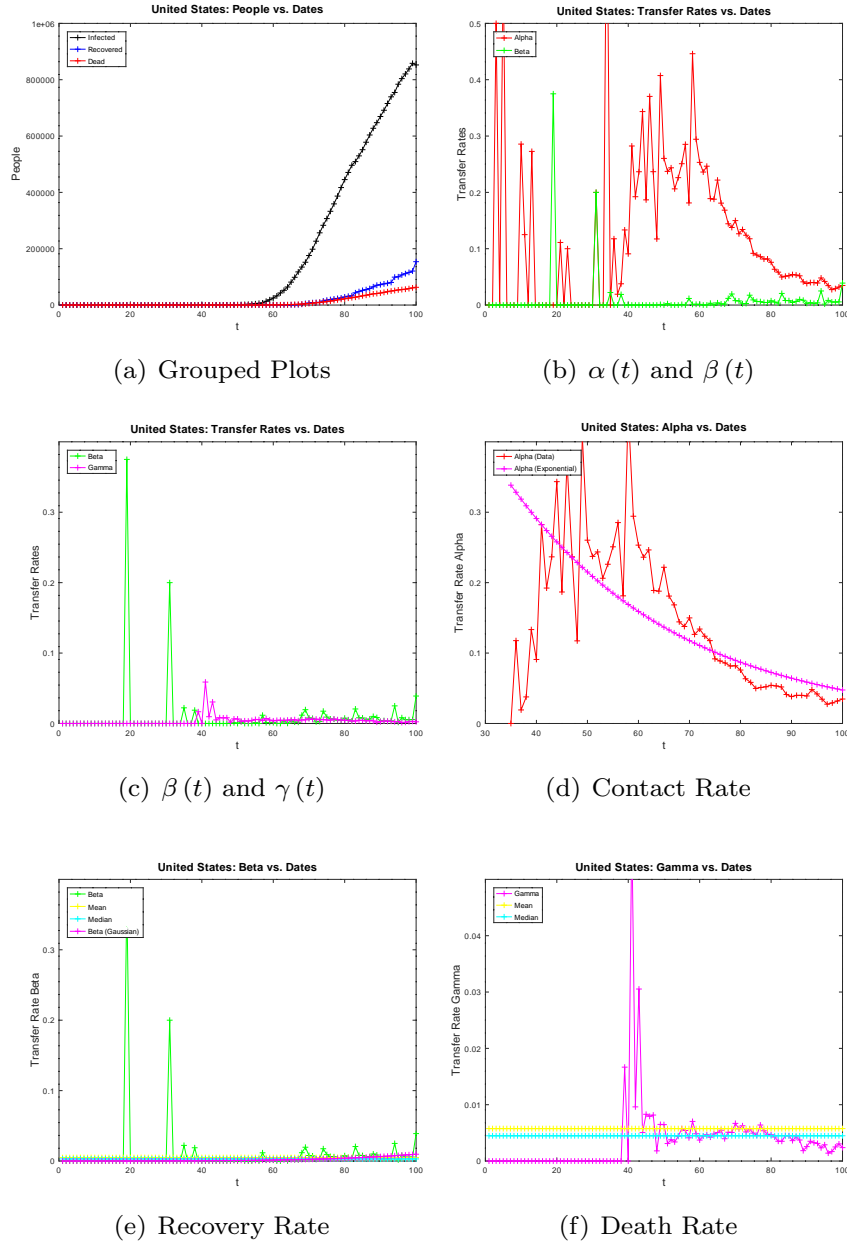
**Figure 12.** Results for our time-discrete parameter identification SIRD model. (a) Plots of processed data for infected people, (cumulative) recovered people and (cumulative) dead people at time $t$. (b) Plots of the time-varying transfer rates $\alpha(t)$ and $\beta(t)$ from our identification algorithm. (c) Plots of the time-varying transfer rates $\beta(t)$ and $\gamma(t)$ from our identification algorithm. (d) Plots of time-varying contact rate $\alpha(t)$ and a parametric approximation with a decaying exponential function. (e) Plots of time-varying recovery rate $\beta(t)$, its mean and median and a parametric approximation with a Gaussian function. (f) Plots of time-varying death rate $\gamma(t)$, its mean and its median.